引用格式：HAO K, HUO C X, YU S, *et al*. Corrosion Resistance Mechanism of TaC-Coated Graphite in High-Temperature Silicon-Containing Steam Environments[J]. Materials China, 2026, 45(2): 155-162.

Corrosion Resistance Mechanism of TaC-Coated Graphite in High-Temperature Silicon-Containing Steam Environments

Kui HAO, Caixia HUO, Shuo YU, Jianxin TU, Le SUN, Maolan YU, Ruicheng BAI, Fangzhou ZHANG, Aijun LI, Haoran LI
(School of Materials Science and Engineering, Shanghai University, Shanghai 200444, China)

Abstract: High-purity graphite is extensively utilized in the semiconductor industry. Enhancing its corrosion resistance is crucial for reducing the manufacturing costs of the third-generation semiconductors. In this study, a continuous and dense TaC coating was fabricated on the surface of graphite using CVD method. The corrosion resistance and mechanism of the coating were investigated in a high-temperature steam environment. This environment involved temperatures exceeding 2200 K and the erosion of the coating by Si-containing mixed steam flows. The results indicated that the corrosion in the affected areas was primarily due to chemical reactions, characterized by the formation of pores and micro-cracks, whereas failure areas were dominated by mechanical delamination, which led to macroscopic defects. Moreover, the mixed high-temperature steam corrosion of the TaC coating showed preferential selectivity, resulting in a stepped corrosion morphology at the crystalline level. The surface roughness of the samples significantly increased after corrosion, from 0.36 to 5.28 μm, although the surface composition remained largely unchanged. The TaC coating provides a certain level of protection to the graphite substrate, enhancing the service life of graphite components and demonstrating promising application potential.

Key words: TaC coating; CVD; SiC; Si-containing vapor; corrosion
CLC number: TN304; TB304 **Document code**: A **Article ID**: 1674-3962(2026)02-0155-08

1 Introduction

With the development of electronics and optoelectronics, the third generation semiconductor materials represented by SiC, GaN and AlN, have garnered significant attention in applications involving high power, high frequency, intense radiation and high temperature[1, 2]. Currently, SiC is the dominant material among the third-generation semiconductors, and the most mature preparation method is physical vapor transport (PVT). This process involves the decomposition of high-purity powder at high temperatures, with the resulting gaseous species being transported to a seed crystal under an axial temperature gradient to form a single crystal[3-5]. Graphite is widely used in the high-temperature environments essential for preparing the third-generation semiconductor materials, owing to its high-temperature resistance, high thermal conductivity and high purity[6-8]. Therefore, improving the corrosion resistance of the thermal field material is crucial to achieving high-quality SiC wafers and high-reliability, high-performance SiC power devices[9-11].

TaC-coated graphite exhibits superior chemical corrosion resistance compared to bare graphite or graphite coated with SiC[12-14]. This coating significantly improves the control over temperature and impurities during the process. Utilizing TaC-coated crucibles for the production of high-quality SiC wafers and related epitaxial layers can reduce dust contamination from the graphite walls, provide a hard and smooth conductive surface, and enhance the service life and reliability of the crucibles[13, 15, 16]. TaC as a ceramic phase that can withstand ultra-high temperature, has been extensively studied for the preparation of coatings on the surfaces of graphite or C/C composites[17, 18]. However, most research has focused on the anti-oxidation and anti-ablation properties of the coating. Since the application of this coating in the semiconductor field, researchers have paid more attention to the corrosion resistance of the TaC coating. Liu *et al*.[19] investigated the atomic oxygen erosion behavior of C/C and TaC-coated C/C composites,

Received date: 2025-01-03 **Revised date**: 2025-03-03
Foundation item: Shanghai Natural Science Foundation (20ZR1419600)
First author: Kui HAO, Male, Born in 1990, Doctor
Corresponding author: Caixia HUO, Female, Born in 1988, Professor, Email: huocaixia2021@shu.edu.cn
Aijun LI, Male, Born in 1975, Professor, Email: aijun.li@shu.edu.cn
DOI: 10.7502/j.issn.1674-3962.202501002

showing that the TaC coating markedly improved resistance to atomic oxygen flux. After 40 h of exposure, the coated composite retained 16.7% higher strength and showed a 57% lower mass ablation rate than the uncoated material. These results highlight the effectiveness of the TaC coating in protecting C/C composites from atomic oxygen-induced erosion. Nakamura *et al*.[16, 20, 21] developed a methodology for applying TaC coatings to graphite substrates through a process involving wet powder forming followed by sintering. The coated components were subjected to rigorous testing within the context of actual high-temperature industrial processes. These included the growth of AlN and SiC bulk single crystals, as well as the fabrication of SiC devices. The results conclusively demonstrated that the TaC-coated components maintained remarkably low levels of impurity incorporation and surface contamination, thereby validating the integrity and reliability of the TaC layers in high-temperature applications. Fan *et al*.[22, 23] fabricated a TaC coating on the graphite surface using chemical vapor deposition (CVD) method. Through simulation and experimental validation, they concluded that the TaC coating serves a protective and insulating function during the PVT growth of SiC single crystals. This extends the service life of graphite components, improves the uniformity of radial temperature, and suppresses the migration of impurities.

In this study, a TaC coating was deposited onto a graphite substrate via CVD method. The corrosion behavior and failure mechanisms of the TaC-coated graphite were systematically investigated under high-temperature conditions (>2200 K) in the Si-containing steam. Characterization of microstructural evolution and surface morphology, including measurements of surface roughness, was conducted to elucidate the degradation process. Furthermore, the propagation of defects and the subsequent failure progression within the TaC coating were comprehensively examined.

2 Experiment

2.1 Sample preparation

In this study, isotropic graphite (IGS-603) was utilized as the substrate material, with a density of 1.8 g/cm^3 and a thermal expansion coefficient of 4.6×10^{-6}/K. To assess the corrosion behavior and mechanism of TaC coatings under high-temperature conditions (> 2200 K) in the Si-containing steam, a TaC coating approximately 20 μm was prepared onto the surface of graphite discs with a dimension of Φ15 mm×5 mm using CVD method.

Before deposition, the samples were ultrasonically cleaned in ethanol for 30 min, followed by drying and subsequent introduction into the CVD reaction chamber. The deposition process employed a system comprising $TaCl_5$, C_3H_6 and Ar, with $TaCl_5$ acting as the tantalum precursor, C_3H_6 providing the carbon source, and Ar serving as the carrier gas. The reaction was conducted at the temperature of 1600~2000 K for 10~20 h, under a controlled pressure within the reaction chamber that did not surpass 500 Pa. When a mixture of $TaCl_5$ vapor and C_3H_6 gas is introduced onto the sample surface, the principal chemical reactions ensued, which are detailed in equations (1)~(3)[19]:

$$C_3H_6(g)\rightarrow 3C(s)+3H_2(g) \quad (1)$$

$$2TaCl_5(g)+5H_2(g)\rightarrow 2Ta(s)+10HCl(g) \quad (2)$$

$$Ta(s)+C(s)\rightarrow TaC(s) \quad (3)$$

2.2 Corrosion test

To investigate the corrosion behavior and mechanisms of TaC-coated graphite samples under high-temperature mixed-gas conditions, SiC powder was placed at the bottom of the graphite crucible. The TaC-coated graphite samples were positioned on the graphite ledge and supported using the small graphite cone. The system was subjected to the temperature exceeding 2200 K for an extended period of 200 h to simulate the growth environment, as depicted in Fig. 1. Under high temperature, SiC powder was expected to produce a complex gaseous mixture comprising SiC, Si, SiC_2 and Si_2C[8].

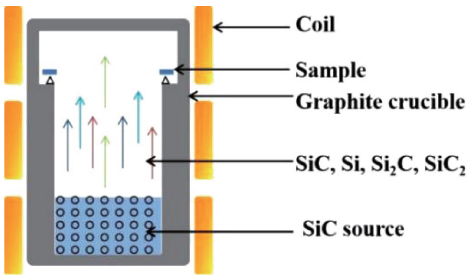

Fig. 1 Schematic diagram of the simulated physical vapor transport (PVT) growth environment for SiC single crystals

2.3 Characterization techniques

The phase characterization of TaC-coated graphites, both before and after corrosion, was conducted using X-ray diffraction (XRD) with Cu Kα radiation. The scanning angles (2θ) ranged from 20° to 80°, with a step size of 0.02°. The morphologies and chemical compositions of the samples were examined through scanning electron microscopy (SEM, JSM6460), complemented by energy dispersive spectroscopy (EDS) for a detailed elemental analysis. To assess the surface

roughness before and after the corrosion process, 3D optical profilometer (S neox 090 V2) was utilized.

3 Results and discussion

3.1 Phases and morphologies of the sample before corrosion

XRD pattern of the TaC coating fabricated on the graphite substrate is depicted in Fig. 2. Analysis of the pattern reveals that the coating is predominantly constituted by two phases, carbon (C) and tantalum carbide (TaC), with no detectable impurities. The 2θ diffraction peak positions for TaC are identified at 34.86°, 40.46°, 58.56°, 70.00° and 73.61°, corresponding to the miller indices of (111), (200), (220), (311) and (222), respectively. The pronounced sharpness of the TaC diffraction peaks is indicative of a high degree of crystallinity and an intact crystalline structure[24]. At the 2θ angle of 26.3°, a diffraction peak attributed to carbon is discernible, with the associated diffraction plane being indexed as (002). It is posited that during the preparation, the carbon source emanating from the pyrolysis of propylene (C_3H_6) partially reacted with tantalum atoms to form TaC, while the remaining carbon did not participate in the reaction and was retained within the coating as free carbon. As a result, the coating exhibits a carbon-rich composition, with the molar ratio of carbon to tantalum surpassing the threshold of 1∶1.

Microstructure of the TaC-coated graphite surface prior to corrosion is depicted in Fig. 3a, with the corresponding higher magnification image presented in Fig. 3b. The micrograph

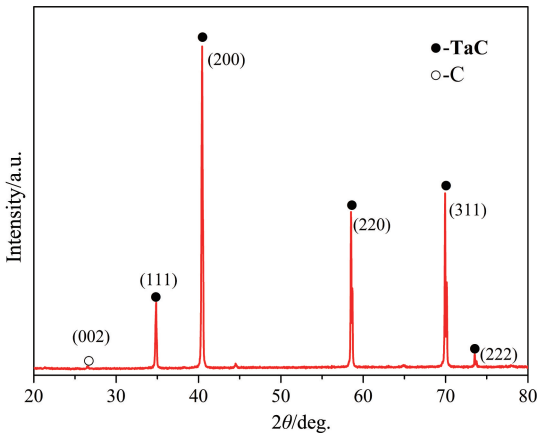

Fig. 2　XRD pattern of the as-deposited TaC-coated graphite before corrosion

reveals that the coating possesses a densely packed microstructure without discernible cracks. In Fig. 3a, discrete black mottled spots are discerned. Elemental analysis at spots 1 and 2 indicates that the coating comprises a TaC matrix enriched with carbon, with the black regions exhibiting an elevated carbon content, represented by an atomic percentage of 86.36% and a mass percentage of 29.59% (Fig. 3c). In contrast, the regions devoid of black spots exhibit a comparatively reduced carbon content, with an atomic percentage of 72.05% and a mass percentage of 14.61% (Fig. 3d). Examination of Fig. 3b reveals that the intergranular boundaries within the coating are smooth, continuous and tightly knit, absent of any pronounced cracks. Nonetheless, minor porosity defects are observable at the convergence of grain boundaries, potentially attributable to the effervescence of gases during the deposition process[24-26].

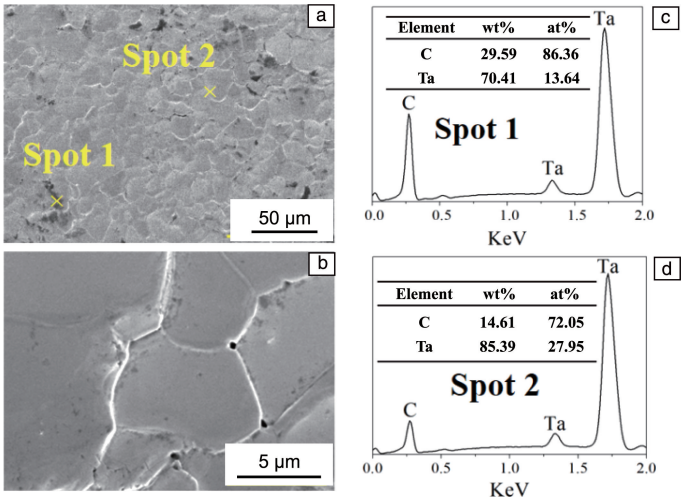

Fig. 3　Microstructure of surface for TaC-coated graphite before corrosion: (a) low magnification SEM image, (b) high magnification SEM image, (c, d) EDS spectra

Fig. 4 shows the grain size distribution within the coating, which was measured statistically based on the maximum contour diameter of the grains. The mean grain size within the sampling area was determined to be 9. 67 μm, with a standard deviation of 3. 32, which denotes minimal data variability and a relatively consistent grain size distribution.

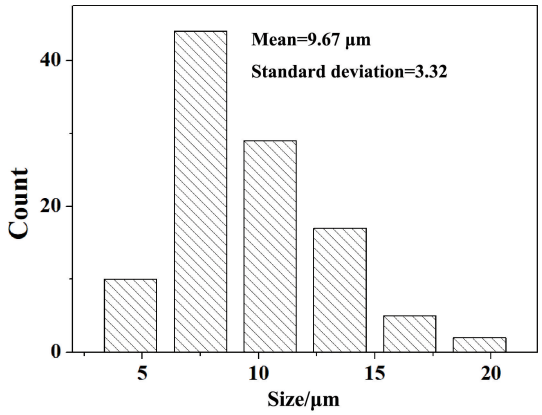

Fig. 4 Grain size distribution of surface for TaC-coated graphite

Fig. 5 demonstrates the application of a 3D profilometer to scrutinize the topographical attributes of the coating's surface. A region approximately 500 μm×500 μm was selected for analysis, revealing a maximum surface height of 2. 84 μm and a local minimum depression height of −3. 52 μm. The surface roughness was measured to be 0. 36 μm, indicative of an overall smooth and even coating with excellent structural integrity.

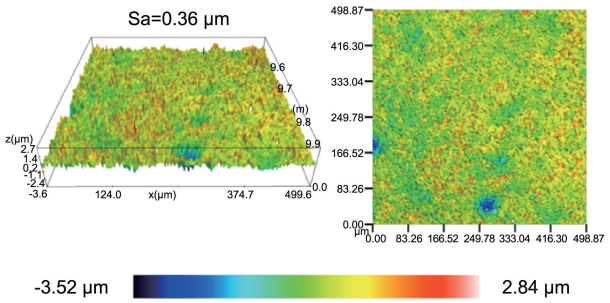

Fig. 5 3D optical profilometer images of surface for TaC-coated graphite before corrosion

Fig. 6a presents the cross-sectional morphology of a graphite sample coated with a TaC layer. The figure indicates a coating thickness of approximately 20 μm. No interfacial delamination is observed, suggesting strong adhesion between the coating and the substrate. The magnified view in Fig. 6b demonstrates that the coating is dense, with no pores, porosity or defects observed within the cross-sectional area. The elemental line scan profiles show that Ta is distributed within a range of 13 ~ 33 μm, which is consistent with the coating thickness of approximately 20 μm measured in Fig. 6a. The elemental mapping of Ta reveals a transition zone enriched with Ta elements, approximately 2 μm thick, at the coating interface[25]. This occurrence is attributed to the presence of pores on the graphite surface. During the CVD process, Ta species, which are partially generated from the decomposition of $TaCl_5$, infiltrate these pores and interact physically or chemically with the carbon constituents of the graphite substrate.

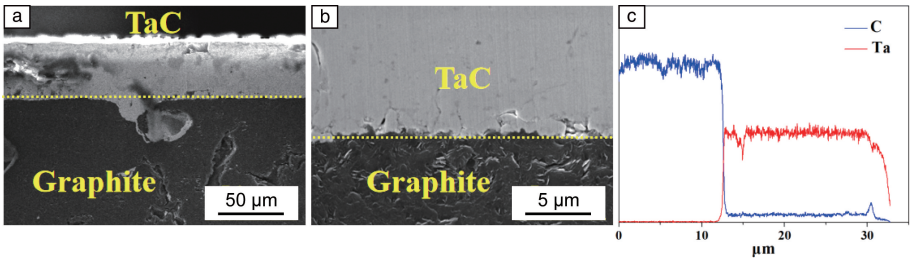

Fig. 6 Cross-sectional morphology of TaC-coated graphite before corrosion (a), relative high magnification (b), line scan spectra (c)

3. 2 Phases and morphologies of the sample after corrosion

The graphite samples coated with TaC, after exposure to high-temperature corrosion above 2200 K in a mixed steam environment (Si, Si_2C, SiC and SiC_2), are analyzed by XRD, with the resulting patterns depicted in Fig. 7. The TaC coating exhibits localized spalling and failure. To elucidate the corrosion mechanism, distinct analyses are performed on the failed and affected regions. As illustrated in Fig. 7, both regions remain consistent with their pre-corrosion states, exhibiting characteristic TaC peaks at 2θ angles of 34. 81°, 40. 42°, 58. 48°, 69. 89° and 73. 49°, corresponding to the diffraction planes of (111), (200), (220), (311) and (222), respectively. Additionally, both regions display C peaks at 2θ angles of 26. 3° and 44. 4°, attributed to the diffraction planes of (002) and (101). The affected region of the coating exhibits cracks and pores, whereas the failure region is characterized by the

coating spalling. This phenomenon results in an enhanced intensity of the C peak within the failure region, and additional SiC peaks appear at 2θ angles of 33.7° and 35.8° within the failure region.

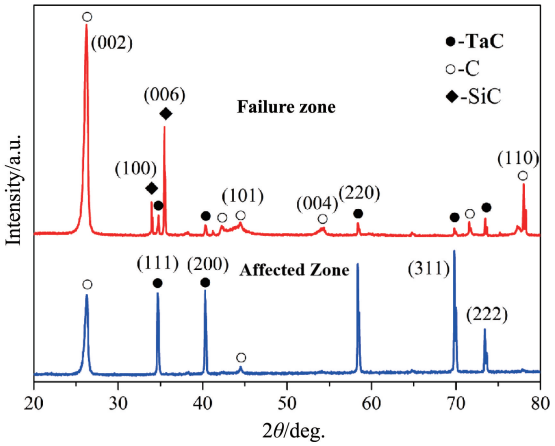

Fig. 7 XRD patterns of TaC-coated graphite surface after mixed steam corrosion including failure and affected zones

The surface micro-morphology of the affected zone after corrosion is shown in Fig. 8. Fig. 8a represents the relatively intact coating, while Fig. 8c depicts the area of the coating with defects. Fig. 8b and 8d are their corresponding high-magnification images. It can be observed from the figures that after 200 h of exposure to high-temperature and mixed-steam corrosive environments, the coating retains a certain level of protective function. Micron-scale cracks and pores appear at the grain boundaries on the surface of the corroded area, and a terraced pattern of corrosion is observed within the grains. The TaC coating exhibits a certain degree of chemical inertness to Si-containing steam at high temperatures, but it can also undergo chemical reactions under certain conditions. This area is primarily characterized by chemical corrosion, as the interface energy at the grain boundaries is relatively high, and the coating itself has pinholes and cracks at the grain intersections. TaC preferentially undergoes chemical reactions with the mixed steam at the grain boundaries, leading to the consumption of the coating. It is possible that the chemical composition and lattice orientation at the grain boundaries have changed, resulting in a terraced pattern of corrosion within the grains. Additionally, due to the difference in thermal expansion coefficients between TaC and the graphite substrate, thermal stress exists in the high-temperature environment. Under the combined action of thermal stress and chemical corrosion, continuous cracking occurs at the grain boundaries, forming cracks.

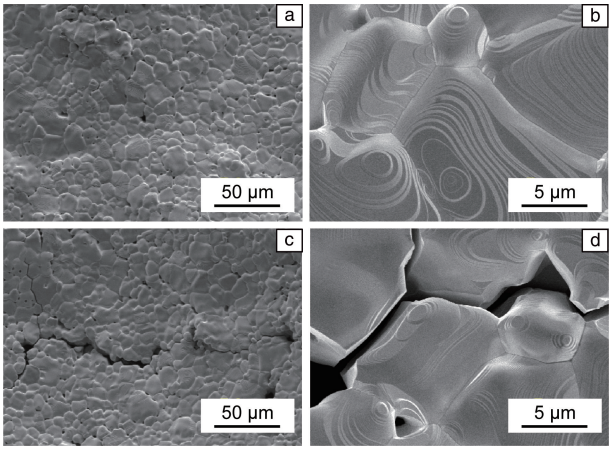

Fig. 8 Microstructure of affected zone for TaC-coated graphite surface after corrosion: (a, b) intact coating and corresponding high-magnification image, (c, d) coating with defects and corresponding high-magnification image

Fig. 9 presents the micro-morphology of the failed zone after corrosion. Fig. 9a is an overall view of the failed area, where area A is the residual TaC coating, area B is the SiC adhesion area, and area C is the graphite layer exposed to the envirenment. Fig. 9d, 9h and 9k, along with their corresponding magnified views Fig. 9e, 9i and 9l, illustrate the micro-morphological characteristics of areas A, B and C. As shown in Fig. 9d, 9e and 9g, the residual TaC coating in the failed area remains intact, with the grains exhibiting a terraced pattern of corrosion. With the continuous flow of Si-containing high-temperature steam over the sample surface, cracks develop in the coating, allowing the steam to penetrate the coating and reach the substrate, shifting the corrosion mechanism to mechanical spalling. Fig. 9h and 9i show that the Si-containing high-temperature steam forms "flake-like" deposits on the sample surface. The elemental mapping at spot 1 shown in Fig. 9h indicates that this area is primarily composed of C and Si elements, with Si content of 57.59wt% (Fig. 9b). Fig. 9k and 9l reveal severe corrosion of the graphite substrate in the failed area. After the TaC coating spalls off, C reacts vigorously with the Si-containing steam at high temperatures, leading to substrate loss. The elemental analysis at spot 2 in Fig. 9k shows that the deeper part of the graphite substrate, after being corroded, is mainly composed of C, with content of 99.12wt% (Fig. 9c). Fig. 9f, 9j and 9m show the distribution of Si, Ta and C elements. Si is essentially distributed throughout the entire area, while Ta is mainly present in the unspalled coating and has not migrated due to chemical reactions.

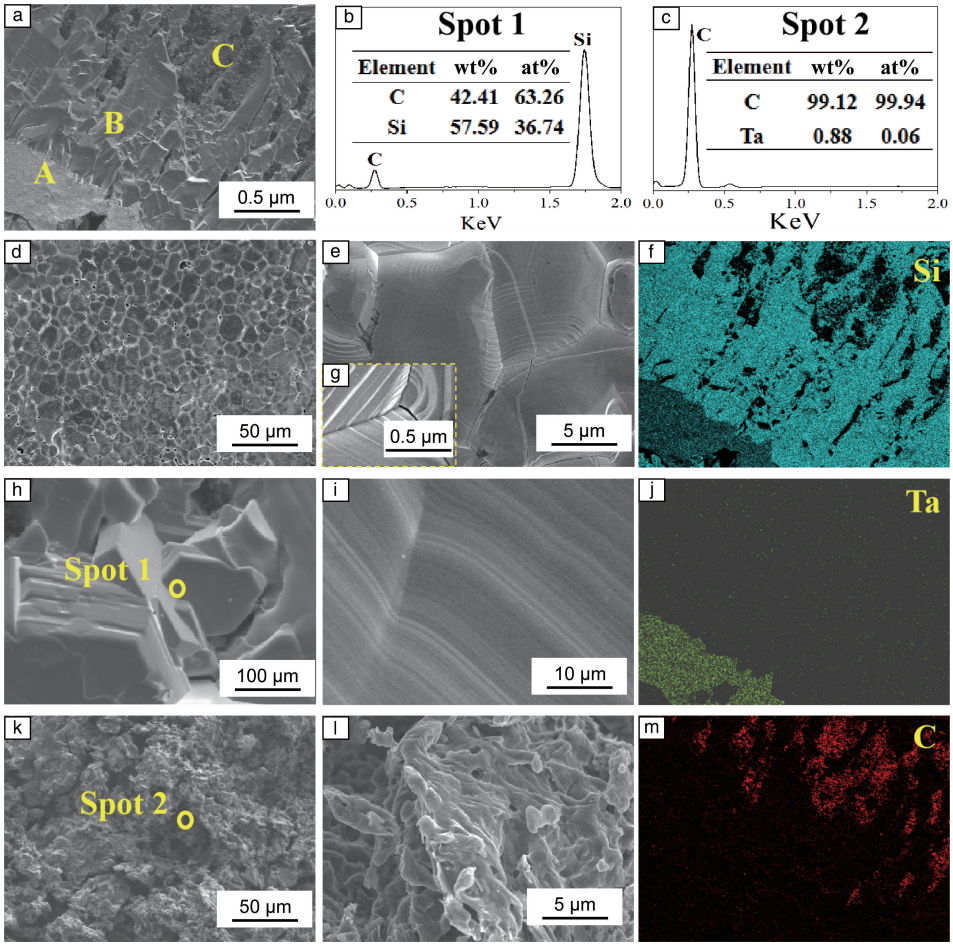

Fig. 9 Microstructure of failure zone for TaC-coated graphite surface after corrosion: (a) general failure area image, (b, c) EDS analysis at spots 1 and 2, respectively; (d, h, k) the views of area A, B and C in Fig. 9a; (e, i, l) corresponding enlarged images of Fig. 9d, 9h and 9k; (g) magnified view of the grain boundary in Fig. 9e; (f, j, m) distribution of Si, Ta and C

Fig. 10 shows the surface roughness of the coating in the corroded area, as characterized by three-dimensional profilometry. The test area was approximately selected as a 500 μm× 500 μm region. The results indicate that this area exhibits a local maximum height of 36.65 μm and a minimum depth of −21.64 μm. The surface roughness increased significantly, reaching a value of 5.28 μm. This increase may be due to the chemical reactions at the grain boundaries during the corrosion process, and on the other hand, it may also be attributed to the difference in thermal expansion coefficients between the TaC coating and the graphite substrate.

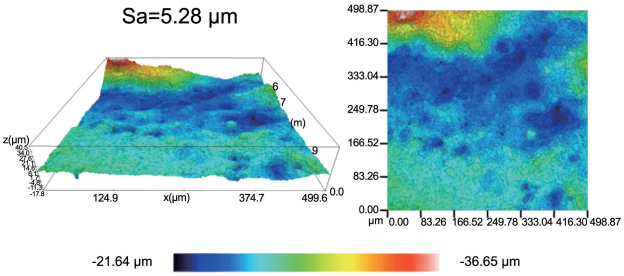

Fig. 10 3D optical profilometer images of surface for TaC-coated graphite after corrosion

3.3 Corrosion mechanism

This article describes the corrosion mechanism of TaC-coated graphite samples when exposed to high temperature exceeding 2200 K and a high-temperature mixed steam produced by the decomposition of SiC powder. Fig. 11 illustrates the corrosion mechanism under the combined influence of high temperature and

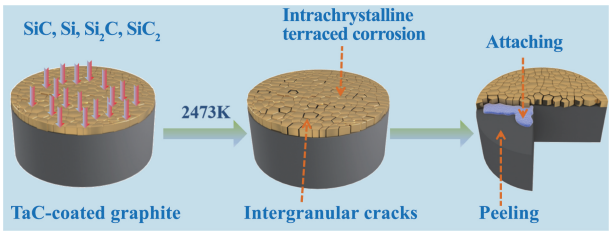

Fig. 11 Mechanism diagram of high temperature mixed steam corrosion of TaC-coated graphite

mixed steam. At the high temperature exceeding 2200 K, SiC powder decomposes into components such as Si, SiC, Si_2C and SiC_2. The mixed vapor stream subsequently induces corrosion on the surface of the TaC coating.

Due to the significantly higher defect and vacancy numbers at grain boundaries compared to within the grains[26], which facilitate the diffusion of high-temperature vapors, TaC coating may undergo the following chemical reactions with Si-containing vapors under high-temperature conditions:

$$TaC+2Si\rightarrow TaSi_2+C \quad (4)$$

$$TaC+2SiC\rightarrow TaSi_2+3C \quad (5)$$

$$TaC+2SiC_2\rightarrow TaSi_2+5C \quad (6)$$

$$TaC+2Si_2C\rightarrow TaSi_2+3C+2Si \quad (7)$$

The chemical reactions occurring at the grain boundaries progressively penetrate into the grain interior, possibly driven by variations in crystallographic orientation or microstructural alterations, manifesting a terraced morphology within the grains[27, 28]. The product $TaSi_2$ detaches from the specimen surface, and in combination with the difference in thermal expansion coefficients between the TaC coating and the graphite substrate, leads to a significant increase in roughness of the affected zone[29, 30]. As the corrosion process progresses, micropores inherent to the coating and microcracks at grain boundaries continuously react with high-temperature vapors, causing the expansion of defects and the formation of cracks. During this phase, the coating still tightly bonds with the substrate, and the corrosion mechanism is primarily chemical reactions.

As the coating cracks expand, Si-containing vapors penetrate into the interior of the coating, forming vapor enrichment at the interface and potentially reacting with the graphite substrate. The corrosion process enters the stage of intense corrosion. The chemical reactions occurring internally provide continuous pathways for the subsequent vapors to enter the material, leading the corrosion to transition to a stage dominated by mechanical spalling, during which the coating essentially loses its protective function for the substrate.

4 Conclusion

The TaC-coated graphite components have been widely applied in the growth of SiC single crystals via physical vapor transport (PVT) process and in semiconductor epitaxial growth. This study investigates the corrosion resistance and the underlying reaction mechanisms of TaC coatings under harsh conditions, providing a reference for subsequent research aimed at improving the coating performance under corrosive conditions. The results of this study indicate that the TaC coating exhibits exceptional corrosion resistance in regions where the coating remains intact and adherent to the substrate. After high temperature environment with Si-containing vapor, the TaC coating still provides protection to the graphite substrate, with no significant changes in the surface composition of the coating before and after corrosion. The roughness increased dramatically from 0.36 μm before corrosion to 5.28 μm after corrosion. Hence, augmenting the coating density and extending the diffusion path length are both expected to significantly enhance the corrosion resistance under such conditions.

References

[1] KIMOTO T, HIYOSHI T, HAYASHI T, *et al*. Journal of Applied Physics[J], 2010, 108(8): 083721.

[2] SHI Y T, REN F F, XU W Z, *et al*. Scientific Reports[J], 2019, 9(1): 8796.

[3] SNYDER D W, HEYDEMANN V D, EVERSON W J, *et al*. Materials Science Forum[J], 2000, 338: 9-12.

[4] GENG W H, SHAO Q Q, WANG Y Z, *et al*. The Journal of Physical Chemistry C[J], 2023, 127(28): 13767-13772.

[5] STEINER J, WELLMANN P J. Materials[J], 2022, 15(5): 1897.

[6] NAKAMURA D. Applied Physics Express[J], 2016, 9(5): 055507.

[7] LUO H, HAN X F, HUANG Y C, *et al*. Crystals[J], 2021, 11: 1581.

[8] LEE D H, LEE H T, BAE B J, *et al*. Materials Science Forum[J], 2014, 778: 26-30.

[9] CHOI J M, LEE C Y, KIM D S, *et al*. Materials Science Forum[J], 2019, 963: 46-50.

[10] CHOI J W, PARK J H, SEO J D, *et al*. Materials Science Forum[J], 2018, 924: 23-26.

[11] HAO K, HUO C X, TU J X, *et al*. Materials Today Communications[J], 2024, 39: 108997.

[12] SCHLESSER R, DALMAU R, ZHUANG D, *et al*. Journal of Crystal Growth[J], 2005, 281(1): 75-80.

[13] HELAVA H I, MOKHOV E N, AVDEEV O A, *et al*. Materials Science Forum[J], 2013, 740: 85-90.

[14] LONG Y, JAVED A, CHEN J, *et al*. Materials Letters[J], 2014, 121: 202-205.

[15] FAN W, QU H, CHANG S I, *et al*. Materials Science Forum[J], 2019, 963: 22-25.

[16] NAKAMURA D, KEISUKE S. Japanese Journal of Applied Physics[J], 2017, 56(8): 085504.

[17] SHEN X S, WANG S, LI W, *et al*. Rare Metal Materials and Engineering[J], 2018, 47(S2): 13-16.

[18] CHEN H R, LIU W, SUN Y N, *et al*. Rare Metal Materials and Engineering[J], 2022, 51(12): 4429-4435.
[19] LIU G, CHENG L, LI K, *et al*. Journal of the European Ceramic Society[J], 2020, 40(3): 642-650.
[20] NAKAMURA D, KIMURA T, NARITA T, *et al*. Journal of Crystal Growth[J], 2017, 478: 163-173.
[21] NAKAMURA D, SHIGETOH K, SUZUMURA A. Journal of the European Ceramic Society[J], 2017, 37(4): 1175-1185.
[22] FAN W, QU H, CHANG S I, *et al*. Materials Science Forum[J], 2019, 963: 22-25.
[23] FAN W, LENNARTZ J, SCHMIDTt-SANE P, *et al*. Materials Science Forum[J], 2022, 1062: 136-139.
[24] CHEN Z K, XIONG X, LONG Y. Applied Surface Science[J], 2011, 257(9): 4044-4050.
[25] FENG G, LI H, YAO X, *et al*. Ceramics International[J], 2019, 45(14): 17936-17945.
[26] CHEN Z K, XIONG X, HUANG B Y, *et al*. Thin Solid Films[J], 2008, 516(23): 8248-8254.
[27] WANG Y, YANG J, LI Q, *et al*. Ceramics International[J], 2022, 48(3): 4158-4164.
[28] LU J H, HAO K, LIU L, *et al*. Corrosion Science[J], 2016, 103: 1-9.
[29] XU Y, ZHENG W, DAI M, *et al*. Journal of the European Ceramic Society[J], 2023, 43(14): 5802-5813.
[30] TAO X, LI X T, GUO L L, *et al*. Surface and Coatings Technology[J], 2017, 316: 122-130.

TaC 涂层石墨在高温含 Si 蒸汽环境中的抗腐蚀机理研究

郝 魁, 霍彩霞, 于 朔, 涂建新, 孙 乐, 俞茂兰, 白瑞成, 张方舟, 李爱军, 李浩然

(上海大学材料科学与工程学院, 上海 200444)

摘 要: 高纯石墨在半导体领域广泛应用, 提高其耐腐蚀性能对降低第三代半导体制造成本具有重要意义。采用 CVD 工艺在石墨表面制备连续致密的 TaC 涂层, 并在高温蒸汽环境下研究其耐腐蚀性能及机理, 包括不低于 2200 K 高温以及含 Si 的混合蒸汽流对涂层的侵蚀。结果表明, 样品受影响区域的腐蚀主要以化学腐蚀为主, 缺陷形式为孔洞和微裂纹, 而失效区域则主要由机械剥离主导, 出现宏观缺陷。混合高温蒸汽腐蚀 TaC 涂层具有择优性, 导致晶内出现阶梯状的腐蚀形态。样品表面粗糙度在腐蚀后显著增加, 从 0.36 增加到 5.28 μm, 而表面成分没有明显变化。TaC 涂层在该环境下对石墨基体具有一定的保护作用, 能提高石墨部件的使用寿命, 有良好的应用前景。

关键词: TaC 涂层; 化学气相沉积; SiC; 含硅蒸汽; 腐蚀